Derivation of Corrections for Ionospheric Faraday Rotation Part 1:Determination of Ionospheric Total Electron Content using Public Domain GPS Data Sets

A. G. Willis[a,*], M. Mevius[b], J. M. Anderson[c], S.O'Sullivan[d], E. Lenc[d], B. S. Arora[e], B. M. Gaensler[d], T. L. Landecker[a]

[a]*National Research Council of Canada, Herzberg, Astrophysics and Astronomy, P.O. Box 248, Penticton, BC, Canada*
[b]*Kapteyn Astronomical Institute, University of Groningen, P.O. Box 800, 9700 AV Groningen, The Netherlands*
[c]*Helmholtz-Zentrum Potsdam, DeutschesGeoForschungsZentrum GFZ, Department 1: Geodesy and Remote Sensing, Telegrafenberg, 14473 Potsdam, Germany*
[d]*Sydney Institute for Astronomy and ARC Centre of Excellence for All-sky Astrophysics (CAASTRO), School of Physics, The University of Sydney, NSW 2006, Australia*
[e]*Curtin Institute of Radio Astronomy, 1 Turner Avenue, Technology Park, Bentley WA 6102, Australia*

Abstract

We have developed a software package that determines the ionosphere total electron content over any location on the Earth as a function of location and time. The software does so by collecting and analysing data from publicly available Global Position System (GPS) data sets. The software may be of interest to both radio astronomers and to ionosphere scientists. Test observations suggest that our analysis gives results consistent with those found by on-site site experiments that used local GPS receivers.

*Corresponding author

Email addresses: tony.willis@nrc-cnrc.gc.ca (A. G. Willis), m.mevius@rug.nl (M. Mevius), anderson@gfz-potsdam.de (J. M. Anderson), s.o'sullivan@physics.usyd.edu.au (S.O'Sullivan), elenc@me.com (E. Lenc), B.Arora@curtin.edu.au (B. S. Arora), bryan.gaensler@sydney.edu.au (B. M. Gaensler), tom.landecker@nrc-cnrc.gc.ca (T. L. Landecker)

Preprint submitted to Elsevier *April 12, 2022*

Keywords:
ionospheric effects, instrumentation: miscellaneous, methods: miscellaneous, polarization, radio continuum: general, telescopes

1. Introduction

New telescopes operating at low frequencies, such as the Murchison Wide-Field Array (MWA)(1) and the Dutch Low Frequency Array (LOFAR) (2) have prompted a new interest in the ionosphere among radio astronomers. The ionosphere, photo-ionized by solar emission and threaded by the Earth's magnetic field, modifies signal phase through its electron content and modifies signal polarization through Faraday rotation in the magnetized plasma. Details from the radio astronomy perspective can be found in chapter 13.3 of (3), section 2.2 of (4) and (5). Faraday rotation observed by a radio telescope contains useful information about the interstellar and intergalacic medium through which the incoming signal has travelled. Consequently, one must remove the ionosphere's contribution to the observed signal in order to derive parameters relevant to regions of astronomical interest.

This paper concerns determination of the total electron content (TEC) of the ionosphere by using publicly available observation data of Global Positioning System (GPS) satellites. (Note that we also use the abbreviations STEC for slant total electron content in a direction away from the zenith, and VTEC for vertical total electron content).

Ionospheric phase effects increase in direct proportion to wavelength. (6) and (4) show that these effects can be handled by modelling a phase screen over the telescope array.

Faraday rotation is a more complex phenomenon which is proportional to wavelength squared. The ionospheric Faraday effect is caused by a combination of free electrons in the Earth's upper atmosphere largely due to photo-ionization from the Sun together with the presence of the Earth's magnetic field. The ionospheric Faraday effect, as seen by an antenna of a telescope array, causes a rotation of the polarized electric vector over an angle χ with respect to the intrinsic polarization position angle of a celestial radio source. The angle χ is related to the wavelength of observation, the Earth's magnetic field $B_{\|}$ along the line of sight (LoS), and the ionosphere electron density by (see (4), equation 11):

$$\chi \propto (\lambda/c)^2 \int_{LoS} B_{\|} n_e ds \tag{1}$$

or

$$\chi = RM\lambda^2 \tag{2}$$

where RM is the rotation measure (usually given in units of $radians/m^2$) The magnetic field is actually a vector quantity and comes toward the observer in the northern hemisphere and goes away from the observer in the southern hemisphere. Consequently the observed RM is usually positive (observed position angle increasing counterclockwise with wavelength) in the north and negative (increasing clockwise) in the south.

In principle, the Faraday rotation angle is a function of source direction and antenna position, but Faraday rotation is usually a large-scale effect and it may have approximately the same value across an entire telescope primary beam field of view (perhaps about one degree). For arrays smaller than a few kilometres, the rotation angle will usually also be the same for all stations. These assumptions reduce the number of independent parameters considerably, but they break down as the observing wavelength gets longer due to the λ^2 effect and increasing field of view, as well as when telescope arrays have longer baselines.

In reality, from the ground we usually cannot directly measure the distribution of the electrons along the line of sight nor directly measure the magnetic field strength as a function of position and direction. In order to calculate a rotation measure, many routines place all the electrons at some "standard" height and attach a magnetic field value from a model of the terrestrial field. In contrast, the software that we describe goes beyond this simple algorithm by distributing the electrons along the line of sight taking into account modern understanding of ionospheric physics, and employs a model of the terrestrial magnetic field that accounts for change of intensity and direction with height.

The original interest of some of the authors in the ionosphere observation and modelling software discussed here was motivated by the POSSUM (Polarization Sky Survey of the Universe's Magnetism) (7) project associated with the ASKAP ("Australian Square Kilometre Array Pathfinder") (8) telescope. ASKAP is a 36 antenna aperture synthesis telescope presently under construction in Western Australia. Each ASKAP antenna will be equipped with a phased array feed capable of forming as many as 36 beams on the sky with an effective field of view of about 30 square degrees. The receiver system is planned to cover a frequency range of 700 to 1800 MHz with a maximum bandwidth for a particular observation of 300 MHz. The target noise after a full synthesis observation of 8 to 10 hours with this bandwidth is 10 μJy per synthesized beam.

The goal of POSSUM is to measure the Faraday rotation of over a million extragalactic radio sources over 30,000 square degrees in order to dramatically improve our understanding of magnetism and the cosmos. In order to accurately determine the rotation measures of the sources, the effects of Faraday rotation in the Earth's own ionosphere must first be removed. The fundamental quantity that can be observed from the ground is the integrated electron density along the line of sight to some reference signal, whereas the magnetic field contribution to Faraday rotation must be derived from a model such as the International Geomagnetic Reference Field (IGRF) field (9).

One of us (Anderson) originally developed a software package to predict and remove such ionospheric effects as part of a European Community funded project ALBUS (Advanced Long Baseline User Software) and he proposed use of this software for POSSUM ionosphere corrections. Over the last two years, our interest in adapting this software for use with other telescopes, especially CHIME (Canadian Hydrogen Intensity Mapping Experiment) (10) has resulted in a package that can be used to determine total electron content (TEC) values as seen from any location on the Earth for a given date / time (since about 2003). The obtained TEC values can be used as input to calculate ionospheric Faraday Rotation measures but may also be useful for ionosphere researchers who would like to obtain detailed variations in TEC as seen for a given location / date

In this paper we focus on computing issues and comparison of the GPS-derived TEC values produced by our software with those obtained by other ionosphere researchers. A second paper (in preparation) will discuss the results of combining the TEC measurements with a magnetic field model to derive rotation measures.

2. Basic Concepts of GPS and Ionospheric Delay

The integrated electron density can be measured because the ionosphere is a dispersive medium and a given signal arrives at a receiving station on the ground later as the observing frequency decreases. A similar effect is seen in pulsar observations - the same pulse arrives later at a lower frequency. Since Global Positioning System (GPS) satellites emit simultaneously signals at two frequencies, 1227.6 and 1575.42 MHz, a measurement of the difference in arrival time of a signal at the two frequencies can be used to derive the electron content between GPS satellites and the observer. Unfortunately GPS satellite signals are subject to numerous sources of error which must be corrected for in order to derive reasonable values for the electron density.

Here we give a very brief summary of GPS ionosphere measurement equations. The interested reader is referred to chapter 3 of (5) for a detailed presentation.

- A GPS Satellite broadcasts at 2 Frequencies in L band
  - L1 = 1575.42 MHz = 19 cm wavelength
  - L2 = 1227.60 MHz = 24 cm wavelength radio astronomers)
- the ionosphere delay $\Delta r = (40.3 * TEC)/f^2$
  - Δr = delay in metres. Ionosphere scientists express delay in metres rather than as a clock offset.
  - TEC (total electron content) is all the electrons in a column with a cross section of $1m^2$ extending from the receiver to a GPS satellite.

TEC is reported in TEC units, where 1 TECU equates to 10^{16} electrons m^{-2}.

- f is frequency in Hz.
- 1 TECU of electrons gives a delay of 0.163 metres for L1 and 0.267 metres for L2
- Every excess of 0.104 metres on L2 - L1 delay corresponds to 1 TECU of electrons

• In an ideal world the only differences in (pseudo)range, P, measured between ground and satellite should be due to the ionosphere delay between L1 and L2

• In theory electron column density in TECU = $(P_{L2} - P_{L1})/0.104m$. In reality observed TECU = $(P_{L2} - P_{L1})/0.104m$ + instrumental delays + multipath + noise

3. Measurement of total electron content (TEC)

There are now many GPS stations scattered around the Earth that are being used for research both on the ionosphere and on plate tectonic movements. Many of these stations report their observations on a daily basis to central data repositories. Data for a given day or time from these stations can then be retrieved by anonymous ftp. An example of such a repository is the Scripps Orbit and Permanent Array Center (SOPAC) (11) at University of California San Diego. We have assembled a list of about 17 repository sites along with positions of some 3300 GPS stations (there is certainly some redundancy) which we use to search for data. In addition there are other sites such as the UK BIGF repository and

GPS Stations within 700 km	
Observatory	GPS Stations with Data
ATCA	23 out of 112
MWA/ASKAP	19 out of 22
MEERKAT	30 out of 34
LOFAR	77 out of 195
GMRT	1 out of 1
VLA	66 out of 95
DRAO/CHIME	125 out of 146
Hat Creek	360 out of 445
OVRO	578 out of 703

Table 1: Observatories and number of potential and active GPS Stations within 700 km Distance

Japanese Geospatial Information Authority (GSI) which will provide data if one submits a written request for research data.

One might note that there is a tendency for GPS stations to proliferate in locations where the study of earthquakes and plate tectonics is important. Table 1 shows the number of GPS stations near some radio telescope sites. Sites in Western North America tend to have a high number of nearby GPS stations (We have not included any Japanese telescope in this survey as we have not tried to get access to the extensive GIS database.) The table shows the number of GPS stations that our data base indicates are within 700 km distance of a telescope and how many of these stations actually provided data in 2013.

CODE (the Center for Orbit Determination in Europe) (12) produces maps of ionosphere Total Electron Content every two hours. The CODE maps make use of only GPS data from the IGS (13) station network scattered around the world (14). The density of these stations is not uniform (the highest average density of stations appears to be in Europe) and is sparse in the locations of both present and planned telescopes such as ASKAP, MEERKAT and the Square Kilometre Array (SKA). Our software modelling system collects data from many 'secondary' GPS stations not used by CODE. The software also collects GPS data produced at 30 second intervals and thus should be able to see ionosphere TEC fluctuations on a more rapid time scale than that derived from the CODE maps.

4. Software Overview

Essentially our software consists of three components - data collection, model fitting, and TEC / RM prediction. The software has a Python layer on top of lower level C and C++ software. The initial version of this software used a Python version less than 2.6 and had to sequentially obtain the name of a GPS data station and then poll up to 17 GPS ftp data servers to find out from which one the data could be obtained. With our expanded list of potential GPS stations, this sequential collection procedure would cause data collection for two or three hundred stations to take many hours.

Since release 2.6 Python has offered a multiprocessing capability. We can now spawn off the ftp data collection step into a sequence of parallel processes as a request for a given GPS station data set has no dependence on requests for data from another GPS station. We adapted the example of using queues to feed a collection of worker processes and collect the results (see bottom of https://docs.python.org/dev/library/multiprocessing.html) . This algorithm has worked extremely well: the data collection process for up to something like 350 potential stations can be completed in about two hours.

If the ftp process finds data for a specified station then the system checks the data quality. Stations may be rejected if the data format is wrong, time sampling is not 30 seconds, or if data from a particular station is not available for the specified time. Secondary data stations are often rejected for reasons similar to the above. Generally about 2/3 of the original list of stations provide data. At this time we believe that the data collection and initial analysis step outlined here are robust and need little if any further work.

Once data collection has been completed, the system fits the GPS data with a model of the ionosphere at the mean position of the telescope. The fitting procedure uses either the International Reference Ionosphere (IRI) (15) or the Parameterized Ionosphere Model (PIM) (16) as an initial estimate.

Further, the software does offer the options to directly generate only an ionosphere model using the International Reference Ionosphere (IRI) or the Parameterized Ionosphere Model (PIM).

Once the fitting procedure is completed, the program calculates total electron content (TEC) and rotation measure (RM) in the direction of observation as a function of time and when finished writes out a report in ASCII format that gives the TEC and RM as a function of time for the specified observation.

We can slice up this output prediction stage into multiple time slices using the same parallel queue algorithm discussed above and then stitch the results into the final report showing the time variations. This parallelism is possible because our output prediction code does not have any dependences on prior time data as would be the case with e.g. a Kalman filter. Further, we noticed that, although GPS data are supplied with 30-second sampling, the output TEC predictions usually exhibit time variations on scales no smaller than five minutes, or even longer. The lower effective time resolution probably arises from the combination of data from many different GPS stations and satellite directions, and is unavoidable. Our conclusion is consistent with that of (17) from early experiments using GPS receivers at the VLA. Accordingly, we have adopted 5 minutes as the default prediction increment for our work.

The net result of our improvements is that a process which originally took about 38 hours in sequential mode to generate a GPS-based ionosphere model for an aperture synthesis observation of 24 hour length can now be completed in about two to three hours. computer.

5. Test Results

Since the fundamental observable from GPS observations is the total electron content (TEC), we have compared TEC derived with our software system with that obtained by other workers. Other workers have mostly been interested in the determination of VTEC, so we have used VTEC in our comparisons,

One of us (Mevius) has written software which takes CODE maps and interpolates the data produced at two hour intervals on to a finer time grid (in the cases investigated here, 300 second increments). Plots of CODE data produced by this software are displayed along with our own GPS data in Figures 1, 2, and 3.

Opperman and co-workers (5) and (18) report VTEC measurements at selected South African locations at various times. In Figure 1 we compare our results with the Louisvale station observations reported by these workers. Louisvale is only 17 km from the standard South African trignet station at Upington. We have generated predictions for Upington for the same dates and times (5 May 2005 and

22 June 2006). We selected the Louisvale/Uppington stations for study because in 2005 they were the closest stations to the MEERKAT / SKA site at a distance of about 257 km. We could obtain data from 195 global and local stations for 2005 and 200 in 2006. Including Upington itself, we had 9 stations within 700 km of Upington in 2005 (and 12 in 2006). Our results (Figure 1) agree well with those shown in (5) and (18).

Figure 1 also reveals interesting trends that occur in other comparisons: (a) The estimates of VTEC derived from CODE IONEX data tend to be higher than those derived by other methods, and (b) VTEC values based on data from stations within 700 km tend to be higher than values derived when we incorporate data from the wider net of IGS GPS stations. Our 'Nearest' plot in Figure 1 agrees well with the fits of (5) and (18). We also find good agreement with the other Louisvale measurements reported by (5).

In preparation for construction of the MWA, a test observation was made with a GPS receiver at the MIT Millstone Hill site in Massachusetts (19). Both our 'All' and 'Nearest' results, shown in Figure 2 (a), agree well with those observed by (19) that are shown at the bottom of the MWA ionosphere web page (20). We have a total of 307 stations in the global fit, of which 134 (44 percent) are local. Once again, we note that the CODE values seem to be on the high side. However, the peak value measured on site is about 2 TEC units above our prediction, intermediate between our prediction and the CODE value.

In this case the 'All' and 'Nearest' fit results agree very well. This may well be because we have a total of 307 stations in the global fit, of which 134 (44 percent) are local stations. We note that the peak value we measure would appear to be about 2 TEC units less than that directly observed at the site. Again CODE

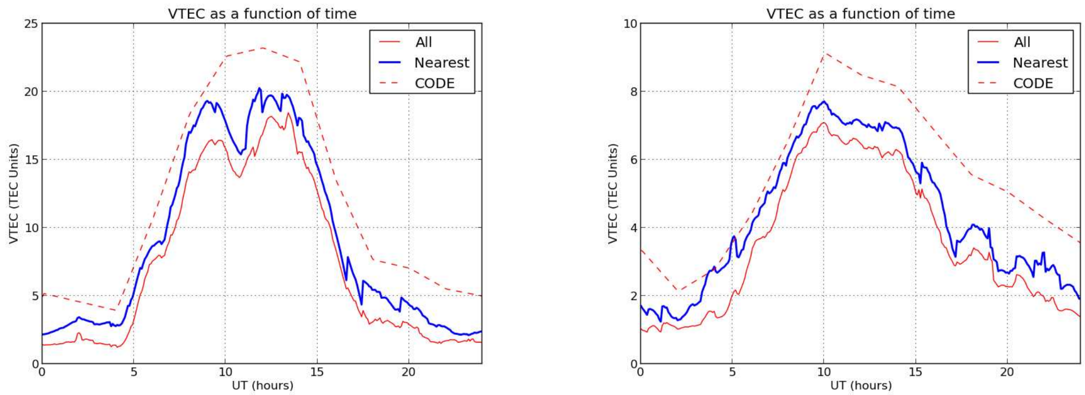

(a) (b)

Figure 1: ALBUS software observation of Upington South Africa VTEC measurements. The 'Nearest' plot shows the fit using local GPS stations situated within 700 km of the site, the 'All' plot show the fit when an additional 184 stations from the GNSS global network are included in the fit. 'CODE' shows the values derived from CODE IONEX maps (a) - May 5, 2005 (b) - June 22, 2006

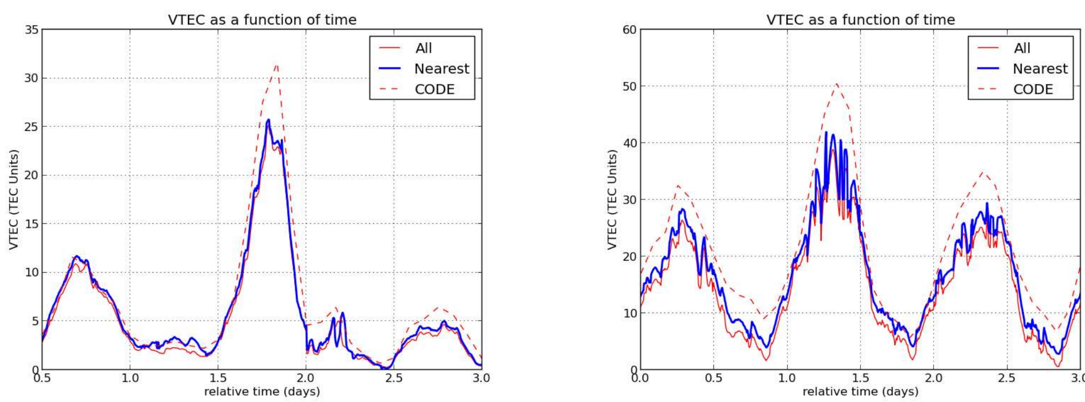

(a) (b)

Figure 2: (a) Determination of Millstone Hill VTEC for the period 12h UT 13 December 2006 to 24 hr UT December 15 2006 (b) Observation of Xiamen, China VTEC for the period 0h UT 23 May 2006 to 24 hr UT 25 May 2006

measurements seem to lie on the high side.

Liu et al (21) report GPS observations at three locations in China in 2006-2007. Their Figure 2 shows VTEC observations covering the period 18 to 27 May 2006 for the three locations. We used our software to generate VTEC for the Xiamen location for the period 23, 24 and 25 May 2006, since there appear to be some fairly rapid TEC fluctuations during those days. Our results in Figure 2 (b) appear to agree well with those of Liu et al. Interestingly, in contrast to the Millstone Hill fit, we could only obtain data from a total of 181 stations, of which just 5 were at distances of less than 700 km.

Figures 1 and 2 show the good agreement that is typical when we compare our results with other work. However, there is one outlier in our data. We compared TEC values for the Australia Telescope Compact Array (ATCA) site at Narrabri (we made observations of the polarization calibrator PKS B1903-802 covering 1100 to 3100 MHz in this period). Figure 3 (a) shows STEC calculated along the line of sight to the radio sources over the 24-hour period. There is a discrepancy of up to 10 TEC units between fits to global and nearby data, with a further offset of 4 to 5 TEC units to the CODE data. Unfortunately it is hard to distinguish between the various predictions on the basis of our radioastronomical measurements because the difference in polarization angle at our lowest frequency of 1100 MHz is only about 2 degrees (Figure 3(b)). The TEC discrepancy would certainly have a marked effect at 300 MHz, where the polarization angle difference between the two solutions would be about 30 degrees.

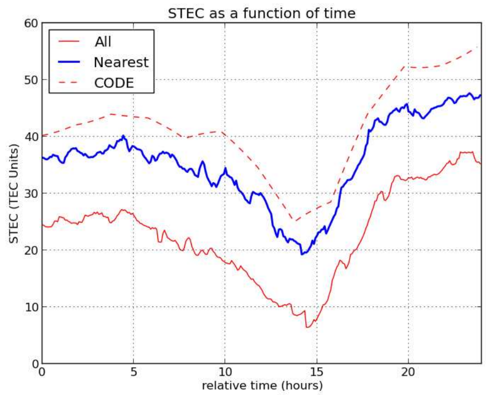

(a)

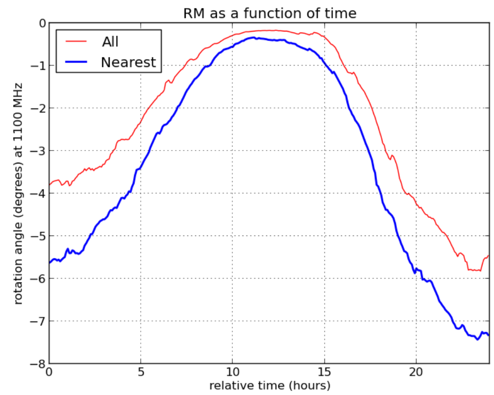

(b)

Figure 3: (a) STEC predictions for the ATCA observation of PKS B1903-802 starting at 04h UT on December 12 2012 (b) Comparison of expected angle change due to calculated RM at 1100 MHz

6. Fitting Errors - Space Weather and Starting Ionosphere Model

The PIM ionosphere modeling system requires space weather information that can be obtained from NASA/NOAA web pages. Unfortunately some space weather data are not posted at the NASA/NOAA sites on a daily basis but may have a lag time of up to several months. Since telescopes such as ASKAP and the SKA may not be able to store raw data for several months while we wait for updated space weather to use for TEC/RM calculations or corrections, it is important to test how the availability of space weather affects the TEC calculations.

As we have described previously we found good agreement between our results and the observations made by Opperman and his co-workers (5) and (18). We took the data that we extracted for Upington, South Africa that corresponded with the five days given in (5) and (18).

Figure 4 (a) shows the difference in derived VTEC with and without space

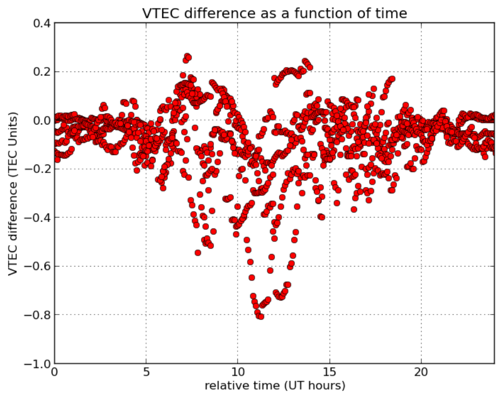

(a)

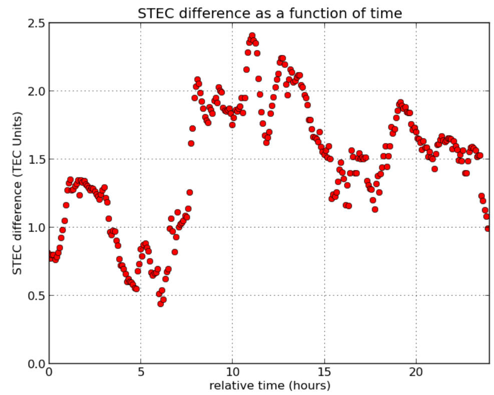

(b)

Figure 4: A display of difference in derived TEC for two different observations (with space weather minus without space weather) (a) Upington (combination of five observations in 2005 and 2006) (b) ATCA December 12 2012

weather for the Upington observations (we have wrapped all observation to fit a 0 to 24 hour UT time frame). The mean difference is -0.08 ± 0.15 TEC units. So any error is small, although the scatter increases in the daytime. On the other hand, our outlier observation of PKS B1903-802 shows a systematic positive offset in TEC, with the difference tending to increase over the course of the observation (Figure 4 (b)).

We also looked at the difference in results when we select as a starting model the PIM (with space weather) ionosphere model vs those obtained with an IRI starting model. Figure 5 shows plots of the differences. The Upington results (again we use all five days) show only a mean offset of about -0.03 ± 0.7 TEC units. However, the ATCA results show a large scatter with an average difference of about -4 TEC units. The ATCA results stand out from our other comparisons, suggesting that there is something odd, perhaps with some of the GPS data we

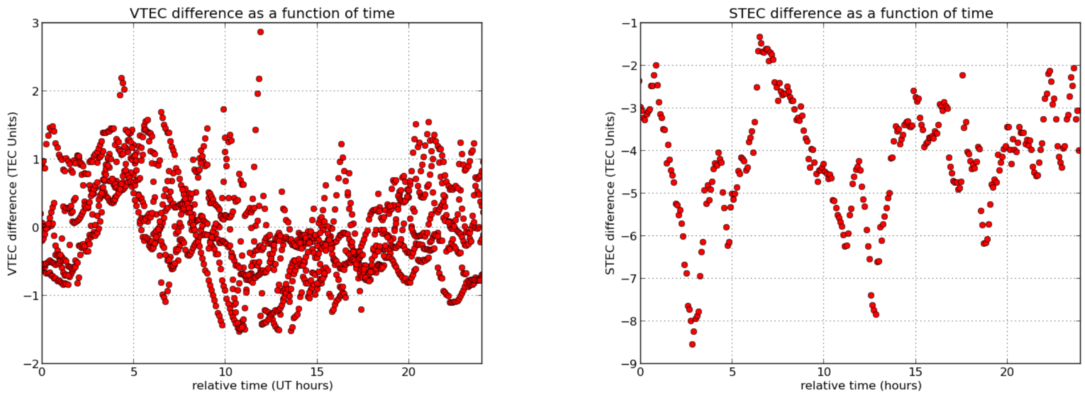

(a) (b)

Figure 5: A display of difference in derived TEC for different starting ionosphere models (PIM - IRI) (a) Upington (combination of five observations in 2005 and 2006) (b) ATCA December 12 2012

collected for this observation.

The rms error in the Upington difference in model fits (PIM vs IRI) is 0.7 TEC units. This is much larger than that found for the case of PIM with vs without space weather of 0.15 TEC units (note the difference in vertical scale between Figure 4 (a) and Figure 5(a)) so it is clear that the model fit is the more significant source of error.

Most of our plots in Figures 1 and 2 show a net bias offset between the different fitting methods. To examine this issue further, we again took the five days worth of Upington data and plotted the differences between fits that just used local data vs fits that included data from the IGSS reference stations. The result is shown in Figure 6. One can clearly see that, although there is considerable scatter, some days are clearly offset from others. The nominal mean and rms of the data is 1.7 $\pm$ 1.1 TEC units. We estimate that this bias scatter increases our

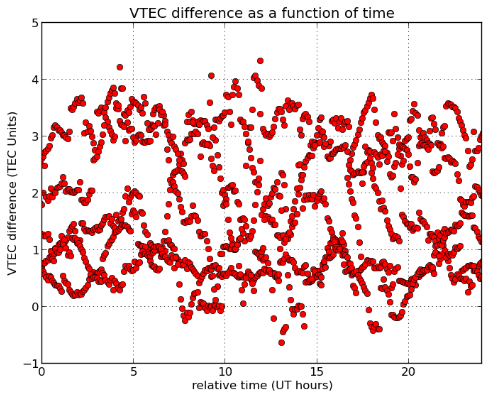

Figure 6: A plot of the biases (local - global) for five days of Upington data in 2005 and 2006

typical measurement uncertainly to about ± 2 TEC units.

7. Conclusions

We have improved the computational efficiency of the ALBUS ionosphere modelling package by modifying the Python control scripts to use parallel processing where possible. We have also expanded the list of GPS receiver stations to include more local sites in addition to CODE / GPS reference sites.

Our TEC results, particularly those derived from using just those stations within a 700 km radius of a specified location, agree well with those values directly observed by a GPS receiver situated at the site. We suggest that the ALBUS software be used in this selection mode. This further decreases computer time as we do not spend time downloading GPS data from some 200 sites remote from the location of interest. We believe that our computed TEC values have an uncertainty of about $\pm$ 2 TEC units.

Throughout this paper we have plotted TEC values derived from CODE (12) maps along with TEC values derived from the ALBUS software. In most cases the agreements are (probably) reasonable with differences in TEC of at most about 4 to 5 TEC units. However it is noticeable that, in general, the CODE results tend to be greater than or equal to the ALBUS results.

If we look at the map of IGS tracking stations (14), we see that the highest density of GPS reference stations used by CODE is in Europe. In other parts of the world the density is generally much lower. It is low in Australia and low in southern Africa. In fact, at present the nearest GPS stations to the ASKAP and MEERKAT array sites that send data to publicly available GPS archives are at about 200 kilometres distance from the sites. The planned SKA telescope will be situated in these two areas, and will have antennas scattered over many hundreds of km in distance. Cosmic magnetism is a major science project for the SKA. Since cosmic magnetism largely depends on accurate polarization measurements for interpretation, we strongly suggest that the SKA set up its own network of GPS receivers to properly monitor local ionospheric conditions.

8. Acknowledgements

We thank George Heald, Charlotte Sobey, and Oleg Smirnov for assistance at various stages of this work. AGW thanks CSIRO, where some of this work was done, for hospitality under the Distinguished Visitor program. AGW, SO'S and EL acknowledge the support of the Australian Research Council through grants FL100100114 and FS100100033, and through the Centre of Excellence for All-sky Astrophysics (CE110001020). Funding was also provided by the National Research Council of Canada and by ASTRON.

References

[1] S. J. Tingay, et al., The Murchison Widefield Array: The Square Kilometre Array Precursor at Low Radio Frequencies, Publications of the Astronomical Society of Australia 30 (2013) e007.

[2] M. P. van Haarlem, et al., LOFAR - the LOw Frequeny ARray, Astron. Astroph 556 (2013) A2.

[3] A. R. Thompson, J. M. Moran, G. W. Swenson Jr, Interferometry and Synthesis in Radio Astronomy, second edition Wiley-VCH, 2004.

[4] O. M. Smirnov, Revisiting the radio interferometer measurement equation II. Calibration and direction-dependent effects, Astron. Astroph. 527 (2011) A107.

[5] B. Opperman, Reconstructing Ionospheric TEC over South Africa using signals from a Regional GPS network, PhD thesis, Rhodes University, Grahamstown, South Africa, available from: eprints.ru.ac.za, 2007.

[6] H. T. Intema, et al., Ionospheric calibration of low frequency radio interferometric observations using the peeling scheme, Astron. Astroph. 501 (2009) 1185–1205.

[7] B. Gaensler, T. Landecker, R. Taylor, POSSUM Collaboration, Bulletin of the American Astronomical Society 42 (2010) 515. [link].
URL `http://www.physics.usyd.edu.au/sifa/possum/`

[8] D. R. De Boer, et al., Australian SKA Pathfinder: A High-Dynamic Range

Wide-Field of View Survey Telescope, Proceedings of the IEEE 97 (2009) 1507–1521.

[9] International Association of Geomagnetism and Aeronomy, Working Group V-MOD, International Geomagnetic Reference Field: the eleventh generation, Geophysical Journal International 183 (2010) 1216–1130.

[10] K. Bandura, et al., Canadian Hydrogen Intensity Mapping Experiment (CHIME) Pathfinder, Proc. SPIE, Astronomical Telescopes + Instrumentation (arXiv:1406.2288), 2014.

[11] SOPAC[link].
URL http://sopac.ucsd.edu/other/sopacDescription.html

[12] CODE[link].
URL http://www.aiub.unibe.ch/content/research/satellite_geodesy/code___research/index_eng.html

[13] J. M. Dow, R. E. Neilan, C. Rizos, The International GNSS Service in a changing landscape of Global Navigation Satellite Systems, Journal of Geodesy 83 (2009) 191–198.

[14] IGS maps[link].
URL http://igs.org/network/complete.html

[15] D. Bilitza, International Reference Ionosphere 2000, Radio Science 36 (2001) 261—275.

[16] R. E. Daniell Jr, et al., Parameterized ionospheric model: A global ionospheric parameterization based on first principles models, Radio Science 30 (1995) 1499–1519.

[17] W. C. Erickson, R. A. Perley, C. Flatters, N. E. Kassim, Ionospheric corrections for VLA observations using Local GPS data, Astron. Astroph. 366 (2001) 1071–1080.

[18] B. D. L. Opperman, P. J. Cilliers, L.-A. McKinnell, R. Haggard, Developement of a regional GPS-based ionospheric TEC model for South Africa, Adv Space Res 39 (2007) 808–815.

[19] J. E. Salah, et al., Ionospheric Structure from GPS and Radar Observations for Radio Array Calibration, American Geophysical Union, Fall Meeting 2007, abstract #SA13A-1062.
URL http://adsabs.harvard.edu/abs/2007AGUFMSA13A1062S

[20] MWA[link].
URL http://www.mwatelescope.org/index.php/science/solar-heliospheric-ionospheric-shi

[21] G. Liu, W. Huang, J. Gong, H. Shen, Seasonal variability of GPS-VTEC and model during low solar activity period (2006-2007) near the equatorial ionization anomaly crest location in Chinese zone, Adv Space Res 51 (2013) 366–376.